Fourier-Transform Near Infrared Spectroscopy (FT-NIRS) rapidly and non-destructively predicts daily age and growth in otoliths of juvenile red snapper *Lutjanus campechanus* (Poey, 1860)

Michelle S. Passerotti[a*], Christian M. Jones[b], Christopher E. Swanson[c], Joseph M. Quattro[a]

[a] University of South Carolina, Department of Biological Sciences, Columbia, SC 29208, USA

[b] National Marine Fisheries Service, Southeast Fisheries Science Center Mississippi Laboratories, Pascagoula, MS 39567, USA

[c] Florida Fish and Wildlife Conservation Commission, Fish and Wildlife Research Institute, St. Petersburg, FL 33701, USA

*corresponding author: mpasserotti@gmail.com

Abstract

Fourier Transform Near Infrared Spectroscopy (FT-NIRS) has shown great promise as a rapid and non-destructive method for predicting age in years from a variety of ageing structures in fish. Herein we assess the utility of FT-NIRS to predict both daily age and otolith weight from whole otoliths of juvenile red snapper *Lutjanus campechanus* collected from the US Gulf of Mexico and southeastern US Atlantic Ocean. Spectral data from whole otoliths (n=153) were collected with a FT-NIR spectrometer while manipulating otolith presentation with an external aperture to maximize signal to noise. Traditional daily age estimates and otolith weights were correlated to spectral data via partial least-squares regression to create age and otolith weight prediction models that were compared across aperture treatments and geographic region. FT-NIRS calibration models using apertured spectra were significantly better at predicting age than models using non-apertured spectra (model rank = 5 and 10, respectively) and yielded predicted age to within an average of six days relative to traditional estimates (R^2 = 0.91, RMSECV = 6.08 days, bias = -0.04). Exponential growth models produced from FT-NIRS-predicted ages ($L_t = 28.3 * e^{0.01t}$) were not significantly different (likelihood ratio $\chi 2$ = 1.05, df = 2, p = 0.591) from those derived from traditional ages ($L_t = 30.7 * e^{0.009t}$). Additionally, FT-NIRS models were capable of predicting otolith weights that were not significantly different from direct measurements (t = 1.746, df = 147, p =

0.082). This study is the first to demonstrate successfully the potential of FT-NIRS to predict daily age and otolith weight in juvenile fishes, as well as the first to manipulate external apertures to optimize signal to noise. These findings support the potential for broad application of FT-NIRS in fisheries biology.

Keywords: age estimation; microincrement; spectroscopy; otolith chemistry; otolith weight

1. Introduction

Estimating the daily age of larval and juvenile fishes as it relates to growth dynamics and environmental correlates is essential to understanding the ecology of fish species, and these data are of particular value for species of management concern. Since Panella (1971) first recognized daily growth increments in the otoliths of juvenile fishes and related them to age, investigations have pursued the use of daily age estimates for reconstruction of environmental, oceanographic, and feeding conditions, as well as to investigate growth and mortality effects throughout larval settlement and ontogenetic shifts (see reviews in Campana and Nielsen, 1985; Sponaugle, 2010). Where incremental deposition is verified as occurring daily for a given species, otolith microincrements are considered a treasure trove of information for determining early life history dynamics and other downstream effects.

Estimating daily age using counts of otolith microincrements is a challenging and time consuming process. Preparing otoliths for daily age estimation requires skill with techniques involving dissection, mounting, and polishing of sometimes microscopic structures, often necessitating the use of cross-polarized light for visualization, in order to produce otoliths with discernable microincrements. In addition, expertise in interpreting microincrements as well as multiple reads and/or readers for the same otolith are necessary to achieve accurate and consistent counts (see Secor et al., 1992; Sponaugle, 2010). In some cases, daily age estimates from microincrements are used in adult fish as well, where more uniform environmental conditions preclude formation of annual growth bands at various stages of adulthood. This is the case with several species of tunas, for which daily age estimates are more

accurate than annual estimates at various stages of adulthood (*e.g.* Williams et al., 2013), presenting further challenges associated with counting large numbers of microincrements over potentially many years of life.

Fourier-Transform Near Infrared Spectroscopy (FT-NIRS) has recently been used to rapidly and non-destructively estimate annual age in several species of fish from scans of various tissues, including otoliths (Table 1). This technique utilizes light from the near infrared region of the electromagnetic spectrum (12,800 – 4000 cm^{-1} wavenumbers, 780 – 2500 nm) to evaluate organic chemical bonds present within a material (Williams, 2008). These bonds vibrate in characteristic ways when irradiated at specific frequencies and thereby absorb light, producing signature absorbance patterns representative of the composition of the sample (Murray and Williams, 1987). Comparison of these absorbance patterns, or spectrograms, among samples as they correlate with other known variables (such as age) can be used alongside multivariate statistical analysis to provide a rapid and non-destructive method of discriminating the variables of interest, e.g., age, from spectral data alone (see Vance et al., 2016 for a review of applications in conservation biology).

Wedding et al. (2014) first demonstrated the utility of FT-NIRS for ageing saddletail snapper (*Lutjanus malacaricus*) from FT-NIRS scans of whole otoliths with a high degree of accuracy and precision relative to traditionally-estimated age in years. Robins et al., (2015) also investigated use of FT-NIRS for annual age estimation in barramundi (*Lates calcarifer*) and pink snapper (*Pagrus auratus*). Recently, Helser et al., (2018) found FT-NIRS could predict age in walleye pollock (*Gadus chalcogrammus*) otoliths with similar precision as traditional methods and, importantly, with resolution to within less than a year relative to traditional annual age estimates. Each of these studies also demonstrated some degree of environmental or regional specificity for otolith spectra. The mechanism behind the FT-NIRS relationship with age, and to a lesser degree to regional or environmental inputs, in otoliths is not explicitly known, but Helser et al., (2018) proposed the accumulation of covalent organic bonds associated with proteins

in the otolith organic matrix as one possibility for further research. One drawback of the FT-NIRS approach is the dependence on traditional age estimates (and therefore any inaccuracies implicit in the technique) for the calibration of a species-specific model that relates spectral data to age, which is a necessary first-step before spectral data can be used alone to estimate age.

Owing to the promising evidence thus far for use of FT-NIRS to predict annual age from whole otoliths, we sought to investigate the use of FT-NIRS to estimate daily ages from whole otoliths of juvenile fish. Red snapper (*Lutjanus campechanus*) is one of the most valuable finfish species in the southeastern United States, with economic impacts of $28 million from commercial landings and $47 million from recreational activities (NMFS, 2018). In addition to directed fisheries, juvenile red snapper in the Gulf of Mexico are also taken in substantial numbers as bycatch in shrimp trawl fisheries (Gutherz and Pellegrin, 1988; Ortiz et al., 2000; Gazey et al., 2012). As such, species monitoring and stock assessment activities for red snapper are substantial and include a large effort focused on the determination of age from otoliths. Studies of juvenile red snapper life history have confirmed daily growth band deposition in otoliths (Szedlmayer, 1998; Rooker et al., 2004), and others have documented regional and habitat-related differences in abundance, growth, and mortality which, when related to daily age estimates, provide valuable insights for management (Workman et al., 2002; Rooker et al., 2004; Patterson et al., 2005; Jones, 2013; Powers et al., 2018). Therefore, red snapper is a worthwhile model species with which to evaluate FT-NIRS as a rapid and non-destructive method of predicting daily age from scans of whole otoliths.

Given the importance of age estimation to fisheries management, the challenges associated with obtaining traditional daily age estimates from otoliths, and the potential for FT-NIRS to improve efficiency of daily age estimation, we investigated the utility of FT-NIRS for estimating daily ages in juvenile red snapper. The objectives for this study were to 1) determine feasibility of using FT-NIRS to estimate daily age from whole otoliths of juvenile red snapper, 2) compare sample presentation methods

for optimizing FT-NIRS prediction results, 3) evaluate equivalence of traditional and FT-NIRS generated ages via growth model analysis, and 4) examine factor loadings of resulting FT-NIRS models for potential underlying sources of spectral variation with age.

2. Methods

2.1. Traditional age estimation

Whole otoliths of juvenile red snapper were obtained from archival samples, whose corresponding paired otolith was aged via traditional methods as described in Jones (2013) and Swanson et al., (in prep). Otoliths from the Jones (2013) study were collected from the US Gulf of Mexico off the Texas coast between 2006 and 2008, while those from the Swanson et al., study (in prep) were collected in 2015 and 2016 off the Florida coast in the Atlantic Ocean. For both studies, estimation of daily ages was carried out by a single reader using two independent counts of increments. In cases where independent counts did not agree but were within 5% CV (Swanson et al., in prep) or 10% CV (Jones, 2013), the counts were averaged to obtain a final age estimate. For counts outside of these respective CV limits, a third count was made and the two counts with CVs within the respective limits were averaged to obtain a final age estimate. Age estimates with CV >10% between the closest two counts were excluded from analysis in all studies. For the purposes of the current study, final increment ages reported in Jones (2013) and Swanson et al. (in prep) are referred to as “traditionally estimated” ages that were subsequently used to inform the FT-NIRS prediction model and to produce “FT-NIRS predicted” ages.

2.2. FT-NIRS

NIR spectral data were acquired using a Bruker Matrix-I Near Infrared Spectrometer with a 22-mm diameter sample window and OPUS 7.8 software (Bruker Scientific, Billerica, MA). Whole otoliths, which had previously been cleaned with water and stored dry for archiving, were first scanned by placing them directly on the center of the sample window, convex side down, conventionally

positioned so that the rostral axis of the otolith was horizontal in relation to the sample window (e.g., see Wedding et al., 2014; Robins et al., 2015; Helser et al., 2018). A 19-mm gold-coated transflectance stamp was placed over the top of each positioned otolith to standardize the path length of NIR incident light. A total of 64 spectral scans were acquired for each otolith in each sample presentation (with and without aperture) at a frequency of 16 cm^{-1} along the entire NIR spectrum (3600 – 12000 cm^{-1}). Scans were averaged to produce a single representative spectrogram for each sample in each presentation. Each representative spectrogram took approximately 30 seconds to produce.

Due to the small size of the otoliths in question (approximately 1.5 – 7.0-mm at the widest point), standardizing the presentation of the otoliths on the sample window was a challenge, and we hypothesized that excess stray light might confound results. As such, we designed a custom aperture fitted over the top of the sample window to constrain the light field and facilitate a standardized positioning of otoliths. The custom aperture was made using a 28-mm diameter white Teflon (PTFE) disc of 0.1-mm thickness (US Plastic Corporation, Lima, OH), through which a 2-mm hole was drilled in the center. The disc was laid directly on top of the sample window so that the aperture hole was centered (Figure 1), and was secured around the edges with masking tape. Otoliths were positioned on the Teflon aperture identically to the first trial, so that the convex apex of the otolith was in direct contact with the sample window via the aperture hole, and the transflectance stamp was again placed over the top. Scans were repeated as described above.

2.3. Data Analyses

All spectral data analysis was conducted using the OPUS software suite (version 7.8, Bruker Scientific). Spectrograms for all samples from both presentation trials were first inspected visually for obvious anomalous or overly noisy spectra. Those that were obviously aberrant based upon visual inspection and could not be rectified by rescanning were removed from the analysis (n = 6). Of the

archival otoliths available for this study, we chose to exclude those with estimated ages greater than 120 days in order to constrain the error surrounding traditional age estimates, as well as to standardize the age ranges of the two regional sample groups. Remaining spectrograms (n = 153) and their corresponding, previously estimated increment ages were modeled using partial least squares regression (PLSR). Background and details for statistical analysis of NIR spectral data related to otolith age, including PLSR, are well described in Wedding (2014) and Helser et al., (2018). Briefly, multivariate spectral data were fitted to traditionally-estimated otolith ages using PLSR, resulting in a calibration model putatively capable of generating a FT-NIRS-predicted age from spectral data alone. After the initial model was fitted, wavenumber selection as well as data preprocessing treatments were trialed to determine treatments and wavenumber ranges that minimized root mean square error (RMSE) of predicted ages. For this study, we determined that a first derivative Savitsky-Golay transform (17 smoothing points, polynomial order = 2) as well as vector normalization (SNV) of mean-centered data with wavenumber selection of 7506 – 4242 cm^{-1} minimized RMSE for all age models. For otolith weight models, the wavenumber ranges selected were 7506 – 6101 cm^{-1} and 4649 – 4242 cm^{-1} with a first derivative Savitsky-Golay transform (17 smoothing points, polynomial order = 2) applied. Models were evaluated using a "leave one out" method of cross validation, whereby calibration models were produced with one sample left out and that sample subsequently tested against the model for goodness of fit. This was repeated, in turn, with each sample tested against the calibration model until all samples had been cross-validated and goodness of fit judged based on the R^2 (coefficient of determination), RMSECV (root mean square error of cross validation), and RPD (residual prediction deviation) values. Due to small sample size for our regional models, within-region samples were not split into separate calibration and validation sample sets, as small sample sets might promote over-confidence in validation models (Williams, 2013). For the regional "combined" models, which had more than 120 samples, we

split the samples into calibration and validation sets for a more robust measure of the predictive capability of the calibration model selected.

Prior studies have sometimes demonstrated measurable differences in NIRS predictive capabilities among different populations of the same species, possibly arising due to differences in water chemistry, condition, or growth rate (Wedding et al., 2014; Robins et al., 2015; Helser et al., 2018). For this reason, we evaluated each regional sample set individually as well as combined into a single calibration model. We also evaluated the effect of the Teflon aperture on model fit for each data set. Best models were selected based upon improvements to R^2, RMSECV, RPD, and rank (number of model factors) over other models.

Equivalence of NIRS-predicted ages to traditionally-estimated ages was evaluated by modeling each age estimate relative to fish standard length (SL, mm) using a maximum log likelihood method (Haddon, 2001), which determined that exponential growth models provided the best fit to the length-at-age data. We tested for significant differences between resulting growth models using a likelihood ratio test (Chen et al., 1992; Haddon, 2001). Length-at-age models were of the form $L_t = L_0 * e^{kt}$, where L_t = body length at age t, L_0 = length at hatch, k = instantaneous rate of growth, and t = age in days.

As a means of evaluating the potential underlying causation of the FT-NIRS-age relationship, we sought to examine the capability of FT-NIRS to predict otolith weight. Otolith weights were collected to the nearest milligram using a Mettler Toledo microbalance (Columbus, OH), and weights were correlated to spectral data via PLSR, wavelength selection, and data preprocessing as outlined for age models above. Factor loadings from FT-NIRS otolith weight models were compared to those of FT-NIRS age models to determine if age-related spectral differences were driven by an otolith weight-age relationship. Equivalence of NIRS-predicted versus directly measured otolith weights was tested using Student's paired t-test on log-transformed weights, due to non-normality of raw otolith weight data (Zar,

1999). Growth model analyses were performed in Microsoft Excel 2016; all other statistical analyses were performed in R (Version 3.4.3 "kite-eating tree", 2017).

3. Results

FT-NIRS spectrograms for a total of 153 otoliths were used to evaluate prediction of daily age and the effect of the Teflon aperture (Atlantic: n = 64, age range 39 – 112 days, mean ± SD = 91.5 ± 19.5 days; Gulf of Mexico: n = 89, age range 39 – 120 days, mean ± SD = 74.4 ± 18.4 days; Figure 2 and Table 2). Overall, FT-NIRS calibration models predicted age well, but there was a strong, positive effect of the Teflon aperture on RMSE and model fit. All models predicted age to within 7.5 days or less relative to traditional ages, on average, based on RMSECV and RMSEP values. Data from Atlantic red snapper otoliths resulted in better prediction models than those from the Gulf of Mexico, especially in terms of model rank. However, the best models both with and without aperture came from the combined region data set, likely due to the increased sample size and thus modeled variability for the calibration. For non-apertured spectra, the Combined model improved R^2 and RPD over both regional models, although the rank and bias increased. However, the Combined Teflon model was an improvement over all other models for R^2, RMSECV, and RPD. Splitting the combined data set into a calibration/validation set was not detrimental to the predictive capability of the calibration model, and the validation model produced the best fit of all the age prediction models in terms of R^2, RMSEP, and RPD, predicting age to within less than 6 days relative to traditional ages for the majority of samples (Figure 3). The Coefficient of Variation (CV) for comparing FT-NIRS-predicted ages versus traditionally estimated ages was 4.3%, which is less than the 5% CV threshold for precision typically considered acceptable for ages generated from traditional methods (Morison et al., 1998; Campana, 2001).

Length at age models fitted using traditional versus FT-NIRS predicted age estimates produced the following exponential growth models (r^2, residual squared error):

Traditional Age: $L_t = 30.7 * e^{0.009t}$ (r^2=0.592, RSE=0.93)

FT-NIRS Age: $L_t = 28.3 * e^{0.01t}$ (r^2=0.661, RSE=0.86)

Models did not differ significantly from one another ($\chi 2 = 1.05$, df = 2, p = 0.591; Figure 4), suggesting the FT-NIRS predicted ages are not significantly different from traditionally estimated ages for this sample set.

FT-NIRS calibration and validation models successfully predicted otolith weight to within a milligram or less for most otoliths, with excellent fit approximating a 1:1 relationship based on R^2, RPD, and bias metrics (Figure 5). FT-NIRS predicted otolith weights (mean ± SD = 0.0165g ± 0.0086g) did not differ significantly from directly measured weights (mean ± SD = 0.0163g ± 0.0085g; t = 1.746, df = 147, p = 0.082), suggesting FT-NIRS predicted otolith weights are equivalent to directly measured otolith weights for this sample set.

Use of the Teflon aperture improved the fit of FT-NIR age prediction models, especially with regard to the rank of the calibration models, and reduced RMSECV by 10 – 16% relative to models using non-apertured spectra (Table 2). The resulting spectral signatures of otoliths scanned with the aperture were different than those scanned without it, presumably due to the interaction of the Teflon with NIR light (Figure 2). However, evaluation of the spectral regions most important to the respective Combined calibration models, as identified from the composite PLSR loadings (Figure 6A), show that the regions that were most influential (i.e. highest amplitude in positive or negative direction) for model results are similar between aperture and non-apertured models, although the relative amplitude of peaks was different in most cases due to reduced variation in the Teflon spectra. This indicates that the use of the aperture did not change which putative molecular bonds contributed to the modeled relationship with age, but instead enhanced the signal to noise ratio to improve resolution around informative regions.

Loadings for factor 1 (describing the majority of the variance explained for each respective model) of age and otolith weight models overlapped in range and amplitude at various points (Figure 6B); however, specific differences are also evident. A large portion (6100 – 4650 cm^{-1}) of the informative range for age was not included in the model for otolith weight. Additionally, the loadings for the peak centered near 4350 cm^{-1} were in opposite directions for the age model (positive) versus the otolith weight model (negative), indicating opposite associations of this spectral band to the respective predictive models.

4. Discussion

Previous studies on the use of FT-NIRS to predict age in otoliths have demonstrated capabilities in age estimation on an annual scale (Table 1). This study is the first to demonstrate the capability of FT-NIRS to predict age on a daily scale from juvenile fish otoliths, as well as the first published use of an aperture for improving otolith presentation to the spectrometer. Our results indicate that FT-NIRS provides a rapid, non-destructive method of accurately estimating daily age parameters but also otolith weight from whole juvenile otoliths, which has broad implications for fisheries applications and management. The ability of FT-NIRS to also predict otolith weight is also highly relevant to the further application of FT-NIRS in fisheries management, because examining the mechanism behind this capability helps shed light on the drivers of the FT-NIRS: age relationship.

Root mean square error of cross validation (RMSECV) is generally the primary diagnostic parameter, amongst others, used to select best fit FT-NIRS calibration models, where minimizing the RMSECV value is desired to achieve the highest precision of FT-NIRS predicted ages to traditional ages. However, evaluating RMSE values as a percentage of the dependent variable range gives a more standardized way to evaluate resolution and assess error across models of different ranges (Couture et al., 2016). Of the species investigated for annual age prediction with FT-NIRS in otoliths thus far, the best

age resolution based on RMSECV values was in *L. calcarifer* with an RMSECV of 0.75 years, or 9 months (Robins et al., 2015). Based upon %RMSE, which we calculate here for all previously published NIRS age prediction models in fish (Table 1), the *G. chalcogrammus* age model (maximum age = 15 years) has the best age resolution at 5.2%, to which our daily age calibration model %RMSE (6.08 days/120 days maximum age = 5.1%) is equivalent despite a much smaller sample size for daily ages. While a threshold RMSE value for accepting FT-NIRS predicted ages as equivalent to traditional ages has not been discussed in published work on otolith ageing to date, the ~ 5% RMSECV resolution presented here and in Helser et al., (2018) are the lowest in the published literature thus far. Given that daily age model resolution improved when regional data sets were pooled and sample size increased, it is likely that larger sample sizes would give even better resolution of daily ages. Thus, it is apparent that FT-NIRS is capable of predicting age at a scale fine enough to be suitable for use in determining daily age from juvenile otoliths.

The use of an aperture to improve resolution of FT-NIRS age prediction in otoliths has not previously been demonstrated. A Teflon aperture has, however, been used in other applications as a means to increase resolution by reducing unwanted background exposure and improve consistency of sample presentation to the spectrometer. Min and Lee (2005) used a Teflon sheet of 3.175 mm thickness with aperture of 25 mm to reduce background interaction and standardize positioning of citrus leaves on the sample window for NIR spectroscopy to predict nitrogen content. That study also provided a correction factor to be applied to apertured-spectra in order to correct for Teflon-induced changes to absorbance signatures. This step was not necessary in our study as we did not seek to integrate spectra obtained both with and without the aperture into a single calibration model. Our results suggest that experimentation with sample presentation is important in pursuit of new applications of FT-NIRS in fisheries, especially when dealing with small samples, and that sample presentation is likely a considerable source of variation among spectrometers and laboratories. When the sample is small

relative to the sample window, it appears excess background signal can negatively impact calibration results. When using an aperture, care should be taken to properly account for its impact on spectral patterns and, if necessary, correction factors should be calculated to allow for integrating apertured and non-apertured data. The aperture used in this study was not large enough to permit scanning of the entire otolith for the largest otoliths in our sample set. As such, it might have been more advantageous to use successively larger apertures that scale with individual otolith size. However, minute differences in the characteristics of each aperture are unavoidable and could likely be a considerable source of error; for this reason we did not manipulate aperture size per se in this study. There exist telescoping aperture fittings for use with NIR spectrometers that could overcome this concern and perhaps provide even better resolution of daily ages in small otoliths.

The potential of FT-NIRS to predict otolith weight has not been previously investigated. It seems intuitive that this correlation should exist given the known correlation of otolith weight with age owing to the incremental accretion of growth bands (e.g., Lou et al., 2005). The ability to predict fish length using FT-NIRS has been demonstrated in two species of shark, however, based upon scans of fin tissues (Rigby et al., 2014). Since FT-NIRS measures quantities and types of organic chemical bonds in materials, we expect that at least some of these quantities change in proportion to size as well as with age, although these changes might not necessarily occur in the same magnitude and/or direction.

The capability of FT-NIRS to predict age in juvenile red snapper otoliths does not appear to be solely based upon its ability to predict weight, and this 'decoupling' has manifold implications for fisheries biology. FT-NIRS age prediction models for juvenile red snapper result in better fit and lower RMSE (mean R^2 = 0.91, mean RMSE = 6.00; Table 2) than the best-fit model produced from regression of daily age with otolith weight alone (R^2 = 0.76, RMSE = 10.01). FT-NIRS models were also found to be better predictors of annual age than were otolith weight-at-age models in *P. auratus* (Robins et al., 2015). Examination of the first factor loadings (Figure 6B) for FT-NIRS predictive models for both age and otolith

weight show that, while the overall range of loadings (and thus the areas of the light spectrum with highest importance to the model) are similar between the age and otolith weight models, there are differences in several important regions of the NIR spectrum. The most obvious divergence occurs between approximately 6094-5454 cm^{-1}, a region that factors heavily in the age model but is excluded in the otolith weight model altogether. This region is associated with O-H bonds from absorbed water within the interstitial spaces of the aragonite matrix (5160 cm^{-1}; Gauldie et al., 1998) as well as C-H and N-H bonds possibly originating from the protein matrix (Wedding 2014; Helser et al., 2018). Loadings in opposite directions around 4350 cm^{-1} also suggests there are changes in number or type of these bonds (likely C-H, N-H, or O-H bonds; Roberts et al., 2017; Brown et al., 2011; Brown et al., 2012; Palukuru et al., 2014) occurring with age that are not associated with changes in otolith weight.

Previous studies have examined otolith weight as a more efficient and less biased corollary of age than estimates from enumerated growth bands (Boehlert 1985; Pawson 1990; Worthington et al., 1995; Matic-Skoko et al., 2011 and references therein; Britton and Blackburn, 2014). While most have found otolith weight to have the highest correlation with age among all otolith size measurements, generally otolith weight alone is not entirely discriminatory in its correlation with age (Francis and Campana 2004; Steward et al., 2009). Indeed, multivariate models incorporating several indices of size at age (i.e. otolith weight and fish length; Brander, 1974) tend to be better corollaries of age (Fossen et al., 2003; Francis and Campana, 2004; Francis et al., 2005; Bermejo, 2016; Hanson and Stafford, 2017), which complements our results in suggesting other dynamics are at work in the relationship between otolith characteristics and age. More study in this area is needed, utilizing larger sample sizes and expansion of analyses to include identifying chemical constituents as they relate to age, as well as expanding investigation to include annual age classes, to better understand the dynamics and specific drivers of the relationships between FT-NIRS, otolith chemistry and age, as well as the interaction of these relationships with otolith size.

Daily incremental otolith growth occurs as alternating deposition of a translucent calcium carbonate layer (as twinned aragonite crystals) with an opaque layer of organic protein matrix rich in acidic amino acids (*e.g.* Gauldie, 1999; Morales-Nin, 2000; Hussy and Mosegaard, 2004). While aragonite may be substituted for its polymorphs calcite or vaterite under certain conditions (Gauldie, 1993; Campana, 1999; Parmentier et al., 2007), this substitution is relatively rare and was not observed in otoliths used in this study based on visual inspection. The protein matrix, however, has been shown to change ontogenetically (Morales-Nin 1986a, 1986b) and also varies in composition according to the environment (Campana and Thorrold, 2001; Elsdon et al., 2008; Sturrock et al., 2012; Chang and Geffen 2013). In addition to changes in amino acids relative to age (Morales-Nin, 1986a; 1986b), relative protein content and the ratio of soluble: insoluble proteins have been shown to undergo ontogenetic changes (Hussy and Mosegaard, 2004). Helser et al., (2018) also posited that the accumulation of proteins within the organic matrix was a likely mechanism for age prediction with FT-NIRS spectral data of walleye pollock otoliths. Thus, the protein matrix seems the most likely driver for age-related, but not necessarily weight-related, chemical changes on a daily scale in juvenile red snapper.

The results of our study have broad application to fisheries science as well as the further use of FT-NIRS in management applications. Estimation of hatch date from increment counts in otoliths of larval and juvenile fishes is routinely used in conjunction with other metrics for evaluating fisheries recruitment dynamics over a range of time scales and influencing factors (e.g. Wright and Trippel, 2009; Sponaugle, 2010; Buckley et al., 2010; Johnson et al., 2014). Especially for species like red snapper, which are protracted spawners, the ability to discriminate among cohorts is key when evaluating the role of seasonal and environmental effects on recruitment. Given the time-consuming nature of producing daily increment counts at a production scale, the capability of FT-NIRS to generate age predictions in a fraction of the time and with improved repeatability relative to traditional methods would save significant costs and improve turnaround time for analyses while maintaining standards for age

precision. Beyond larval and juvenile fish, this technique also has application to species that do not deposit easily discernable annual increments but instead must be aged via daily microincrement counts, as has been the case with tuna species such as skipjack *Katsuwonus pelamis*, yellowfin *Thunnus albacares*, albacore *T. alalunga*, bigeye *T. obesus* and Pacific bluefin tuna *T. orientalis* (*e.g.* Williams et al., 2013). The non-destructive nature of FT-NIRS analysis also allows for both otoliths to be available for further study beyond simple age determination and opens opportunities for comparative analyses utilizing destructive techniques. Insights from this study regarding the relationship of FT-NIRS to both age and otolith weight further the discourse related to broader use of FT-NIRS in fisheries applications. The basis of using FT-NIRS for age determination does not lie in knowledge of the underlying chemical constitution of the tissues being analyzed; rather, it simply relies upon detection of small differences in the types and concentrations of various molecular bonds present in the sample relative to age, which could be associated with any number of molecular compounds (Siesler et al., 2002; Helser et al., 2018; Rigby et al., 2018). However, as with any new method, results must be vetted and, ideally, underlying drivers understood so that any potential shortcomings can be identified. Additionally, deeper investigation into age-related changes in structural chemistry may opportunistically provide insights into new primary chemical methods for age determination not previously known to the field. Future work involving FT-NIRS application to fish age should include examination of underlying chemistry as it relates to spectral data in pursuit of understanding on both fronts, as well as continued experimentation to optimize sample presentation and determination of best practices for comparing data and results across spectrometers and laboratories.

Acknowledgements

We extend thanks to Joshua Brennan, Jason Erickson, Irina Benson, Dr. Thomas Helser, and Dr. Michael Myrick for helpful guidance and discussion surrounding FT-NIR methods. Allen Andrews provided insightful discussion about otolith weight and otolith chemistry. Alex Chester provided useful edits to an earlier version of the manuscript.

Funding: This work was supported by South Carolina Sea Grant [R/CF-23], an equipment grant from the College of Arts and Sciences, University of South Carolina, and funds from a SPARC Graduate Research and an ASPIRE-I grant from the Office of the Vice President for Research at the University of South Carolina.

Literature Cited

Boehlert, G.W., 1985. Using objective criteria and multiple regression models for age determination in fishes. *Fishery bulletin*, *83*(2), pp.103-117.

Brander, K. 1974. The effects of age-reading errors on the statistical reliability of marine fishery modelling. In: The Ageing of Fish (ed. T.B. Begenal). Unwin Bros., Surrey.

Britton, J.R. and Blackburn, R., 2014. Application and utility of using otolith weights in the ageing of three flatfish species. *Fisheries research*, *154*, pp.147-151.

Brown, C.P., C. Jayadev, S. Glyn-Jones et al., 2011. Characterization of early stage cartilage degradation using diffuse reflectance near infrared spectroscopy. *Physics in Medicine and Biology,* 56, pp. 2299-2307.

Brown, C. P., A. Oloyede, R. W. Crawford, G. E. Thomas, A. J. Price, and H. S. Gill. 2012. Acoustic, mechanical and near-infrared profiling of osteoarthritic progression in bovine joints. *Physics in Medicine and Biology,* 57, 547–559.

Buckley, L.J., Lough, R.G. and Mountain, D., 2010. Seasonal trends in mortality and growth of cod and haddock larvae result in an optimal window for survival. *Marine Ecology Progress Series*, 405, pp.57-69.

Campana, S.E. and Neilson, J.D., 1985. Microstructure of fish otoliths. *Canadian Journal of Fisheries and Aquatic Sciences*, 42(5), 1014-1032.

Campana, S.E. 1999. Chemistry and composition of fish otoliths: pathways, mechanisms and applications. *Marine Ecology Progress Series*, 188, 263-297.

Campana, S.E., 2001. Accuracy, precision and quality control in age determination, including a review of the use and abuse of age validation methods. *Journal of fish biology*, *59*(2), pp.197-242.

Campana, S.E. and Thorrold, S.R., 2001. Otoliths, increments, and elements: keys to a comprehensive understanding of fish populations? *Canadian Journal of Fisheries and Aquatic Sciences*, *58*(1), pp.30-38.

Chang, M.Y. and Geffen, A.J., 2013. Taxonomic and geographic influences on fish otolith microchemistry. *Fish and Fisheries*, *14*(4), pp.458-492.

Chen, Y., Jackson, D.A. and Harvey, H.H., 1992. A comparison of von Bertalanffy and polynomial functions in modelling fish growth data. *Canadian Journal of Fisheries and Aquatic Sciences, 49*(6), pp.1228-1235.

Couture, J.J., Singh, A., Rubert-Nason, K.F., Serbin, S.P., Lindroth, R.L. and Townsend, P.A., 2016. Spectroscopic determination of ecologically relevant plant secondary metabolites. *Methods in Ecology and Evolution, 7*(11), pp.1402-1412.

Elsdon, T.S., Wells, B.K., Campana, S.E., Gillanders, B.M., Jones, C.M., Limburg, K.E., Secor, D.H., Thorrold, S.R. and Walther, B.D., 2008. Otolith chemistry to describe movements and life-history parameters of fishes: hypotheses, assumptions, limitations and inferences. *Oceanography and marine biology: an annual review*, *46*(1), pp.297-330.

Fossen, I., Albert, O.T. and Nilssen, E.M., 2003. Improving the precision of ageing assessments for long rough dab by using digitised pictures and otolith measurements. *Fisheries Research*, *60*(1), pp.53-64.

Francis, R.I.C.C. and Campana, S.E., 2004. Inferring age from otolith measurements: a review and a new approach. *Canadian Journal of Fisheries and Aquatic Sciences*, *61*(7), pp.1269-1284.

Francis, R.I.C.C., S.J. Harley, S.E. Campana and P. Doering-Arjes. 2005. Use of otolith weight in length mediated estimation of proportions at age. *Marine and Freshwater Research, 56*, 735-743.

Gauldie, R.W., 1993. Polymorphic crystalline structure of fish otoliths. *Journal of morphology*, *218*(1), pp.1-28.

Gauldie, R.W., Thacker, C.E., West, I.F. and Wang, L., 1998. Movement of water in fish otoliths. *Comparative Biochemistry and Physiology Part A: Molecular & Integrative Physiology*, *120*(3), pp.551-556.

Gauldie, R.W., 1999. Ultrastructure of lamellae, mineral and matrix components of fish otolith twinned aragonite crystals: implications for estimating age in fish. *Tissue and Cell*, *31*(2), pp.138-153.

Gazey, W. J., Gallaway, B. J., Cole, J. G., & Fournier, D. A. (2008). Age composition, growth, and density dependent mortality in juvenile red snapper estimated from observer data from the Gulf of Mexico penaeid shrimp fishery. *North American Journal of Fisheries Management, 28*(6), 1828 -1842.

Gutherz, E. J., & Pellegrin, G. J. (1988). Estimate of the catch of red snapper, *Lutjanus campechanus*, by shrimp trawlers in the U.S. Gulf of Mexico. *Marine Fisheries Review, 50*(1), 17-25.

Haddon, M. (2001). 'Modelling and Quantitative Methods in Fisheries.' (Chapman & Hall, CRC Press: Boca Raton, FL.)

Hanson, S.D. and Stafford, C.P., 2017. Modeling otolith weight using fish age and length: applications to age determination. *Transactions of the American Fisheries Society*, *146*(4), pp.778-790.

Helser, T.E., Benson, I., Erickson, J., Healy, J., Kastelle, C. and Short, J.A., 2018. A transformative approach to ageing fish otoliths using Fourier transform near infrared spectroscopy: a case study of eastern Bering Sea walleye pollock (*Gadus chalcogrammus*). *Canadian Journal of Fisheries and Aquatic Sciences, 76*(5), 780-789, https://doi.org/10.1139/cjfas-2018-0112

Hüssy, K. and Mosegaard, H., 2004. Atlantic cod (Gadus morhua) growth and otolith accretion characteristics modelled in a bioenergetics context. *Canadian Journal of Fisheries and Aquatic Sciences*, *61*(6), pp.1021-1031.

Johnson, D.W., Grorud-Colvert, K., Sponaugle, S. and Semmens, B.X., 2014. Phenotypic variation and selective mortality as major drivers of recruitment variability in fishes. *Ecology letters*, *17*(6), pp.743-755.

Jones, C.M., 2013. Growth and mortality of pre and post-settlement age-0 red snapper, *Lutjanus campechanus* (Poey 1860), in the Gulf of Mexico. Dissertation, University of South Alabama.

Lou, D.C., Mapstone, B.D., Russ, G.R., Davies, C.R., Begg, G.A., 2005. Using otolith weight–age relationships to predict age-based metrics of coral reef fish populations at different spatial scales. *Fisheries Research, 71*, 279–294.

Matić-Skoko, S., Ferri, J., Škeljo, F., Bartulović, V., Glavić, K. and Glamuzina, B., 2011. Age, growth and validation of otolith morphometrics as predictors of age in the forkbeard, *Phycis phycis* (Gadidae). *Fisheries research, 112*(1-2), pp.52-58.

Min, M. and Lee, W.S., 2005. Determination of significant wavelengths and prediction of nitrogencontent for citrus. *Transactions of the ASAE, 48*(2), pp.455-461.

Morales-Nin, B.Y.O., 1986a. Structure and composition of otoliths of Cape hake *Merluccius capensis*. *South African Journal of Marine Science, 4*(1), pp.3-10.

Morales-Nin, B., 1986b. Chemical composition of the sea bass (*Dicentrarchus labrax*, Pisces: Serranidae) otoliths. *Cybium 10*(2), 115-120.

Morales-Nin, B., 2000. Review of the growth regulation processes of otolith daily increment formation. *Fisheries Research*, *46*(1-3), pp.53-67.

Morison, A. K., Robertson, S. G. & Smith, D. G. (1998). An integrated system for production fish aging: image analysis and quality assurance. *North American Journal of Fisheries Management, 18*, 587–598.

Murray, I., and Williams, P., 1987. Chemical principles of near-infrared technology. In: Williams, P., Norris, K. (eds) Near Infrared Technology in the Agricultural and Food Industries. American Association of Cereal Chemists, St. Paul, MN, pp 29-31.

National Marine Fisheries Service (2018). Fisheries of the United States, 2017. U.S. Department of Commerce, NOAA Current Fishery Statistics No. 2017 Available at: https://www.fisheries.noaa.gov/feature-story/ fisheries-united-states-2017

Ortiz, M., Legault, C.M. & Ehrhardt, N.M. (2000). An alternative method for estimating bycatch from the U.S. shrimp trawl fishery in the Gulf of Mexico, 1972-1995. *Fishery Bulletin, 98*, 583-599.

Palukuru, U. P., C. M. McGoverin, and N. Pleshko, 2014. Assessment of hyaline cartilage matrix composition using near infrared spectroscopy. *Matrix Biology, 38*: 3–11.

Panella, G., 1971. Fish otoliths: daily growth layers and periodical patterns. *Science*, *173*(4002), pp.1124-1127.

Parmentier, E., Cloots, R., Warin, R. and Henrist, C., 2007. Otolith crystals (in Carapidae): Growth and habit. *Journal of Structural Biology*, *159*(3), pp.462-473.

Patterson, W.F., Wilson, C.A., and Bentley, S.J., 2005. Delineating juvenile red snapper habitat on the northern Gulf of Mexico continental shelf. *In* American Fisheries Society Symposium (Vol. 41, pp. 277-288).

Pawson, M.G., 1990. Using otolith weight to age fish. *Journal of Fish Biology*, *36*(4), pp.521-531.

Powers, S.P., Drymon, J.M., Hightower, C.L., Spearman, T., Bosarge, G.S. and Jefferson, A., 2018. Distribution and age composition of red snapper across the inner continental shelf of the north central Gulf of Mexico. *Transactions of the American Fisheries Society, 147*(5), pp.791-805.

Rigby, C.L., Wedding, B.B., Grauf, S. and Simpfendorfer, C.A., 2014. The utility of near infrared spectroscopy for age estimation of deepwater sharks. *Deep Sea Research Part I: Oceanographic Research Papers*, *94*, pp.184-194.

Rigby, C.L., Wedding, B.B., Grauf, S. and Simpfendorfer, C.A., 2015. Novel method for shark age estimation using near infrared spectroscopy. *Marine and Freshwater Research*, *67*(5), pp. 537-545.

Rigby, C.L., Foley, W.J. and Simpfendorfer, C.A., 2018. Near-Infrared Spectroscopy for Shark Ageing and Biology. *Shark Research: Emerging Technologies and Applications for the Field and Laboratory*.

Roberts, J.J., Motin, J.C., Swain, D. and Cozzolino, D., 2017. A feasibility study on the potential use of near infrared reflectance spectroscopy to analyze meat in live animals: discrimination of muscles. Journal of Spectroscopy, 2017. 10.1155/2017/3948708

Robins, J.B., Wedding, B.B., Wright, C., Grauf, S., Fowler, A., Saunders, T. and Newman, S., 2015. *Revolutionising Fish Ageing: Using Near Infrared Spectroscopy to Age Fish*. State of Queensland through Department of Agriculture and Fisheries.

Rooker, J.R., Landry Jr, A.M., Geary, B.W. and Harper, J.A., 2004. Assessment of a shell bank and associated substrates as nursery habitat of postsettlement red snapper. *Estuarine, Coastal and Shelf Science*, *59*(4), pp.653-661.

Secor, D.H., Dean, J.M. and Laban, E.H., 1992. Otolith removal and preparation for microstructural examination. *Otolith microstructure examination and analysis. Canadian special publication of fisheries and aquatic sciences*, *117*, pp.19-57.

Siesler, H. W., Ozaki, Y., Kawata, S., and Heise, H. M. (Eds) (2002). 'Near-Infrared Spectroscopy. Principles, Instruments, Applications.' (Wiley-VCH Verlag: Weinheim, Germany.)

Sponaugle, S., 2010. Otolith microstructure reveals ecological and oceanographic processes important to ecosystem-based management. *Environmental Biology of Fishes*, *89*(3-4), pp.221-238.

Steward, C.A., DeMaria, K.D. and Shenker, J.M., 2009. Using otolith morphometrics to quickly and inexpensively predict age in the gray angelfish (Pomacanthus arcuatus). *Fisheries Research*, *99*(2), pp.123-129.

Sturrock, A.M., Trueman, C.N., Darnaude, A.M. and Hunter, E., 2012. Can otolith elemental chemistry retrospectively track migrations in fully marine fishes?. *Journal of Fish Biology*, *81*(2), pp. 766-795.

Swanson, C. et al., Spatio-temporal variation in daily growth and size structure of juvenile south Atlantic Red Snapper (*Lutjanus campechanus*). *In prep*.

Szedlmayer, S.T. 1998. Comparison of growth rate and formation of otolith increments in age-0 red snapper. *Journal of Fish Biology, 53,* 58-65.

Vance, C.K., Tolleson, D.R., Kinoshita, K., Rodriguez, J. and Foley, W.J., 2016. Near infrared spectroscopy in wildlife and biodiversity. *Journal of Near Infrared Spectroscopy*, *24*(1), pp.1-25.

Wedding, B.B., Forrest, A.J., Wright, C., Grauf, S., Exley, P. and Poole, S.E., 2014. A novel method for the age estimation of Saddletail snapper (Lutjanus malabaricus) using Fourier Transform-near infrared (FT-NIR) spectroscopy. *Marine and Freshwater Research*, *65*(10), pp.894-900.

Williams, P., 2008. Near-infrared technology-getting the best out of light. A short course in the practical implementation of near-infrared spectroscopy for the user. A short course held in conjunction with the 13th ANISG Conference. Australian Near Infrared Spectroscopy Group, Department of Primary Industries - Hamilton Centre. Victoria, Canada

Williams, P., 2013. Tutorial: Calibration development and evaluation methods B. Set-up and evaluation. *NIR News, 24* (6), 20-24.

Williams, A. J., Leroy, B. M., Nicol, S. J., Farley, J. H., Clear, N. P., Krusic-Golub, K., and Davies, C. R. 2013. Comparison of daily- and annual-increment counts in otoliths of bigeye (*Thunnus obesus*), yellowfin (*T. albacares*), southern bluefin (*T. maccoyii*) and albacore (*T. alalunga*) tuna. *ICES Journal of Marine Science, 70,* 1439–1450.

Workman, I., Shah, A., Foster, D., and Hataway, B. 2002. Habitat preferences and site fidelity of juvenile red snapper (*Lutjanus campechanus*). *ICES Journal of Marine Science, 59*, S43–S50. doi:10.1006/JMSC.2002.1211

Worthington, D.G., Fowler, A.J. and Doherty, P.J., 1995. Determining the most efficient method of age determination for estimating the age structure of a fish population. *Canadian Journal of Fisheries and Aquatic Sciences*, *52*(11), pp.2320-2326.

Wright, P.J. and Trippel, E.A., 2009. Fishery-induced demographic changes in the timing of spawning: consequences for reproductive success. *Fish and Fisheries*, *10*(3), pp.283-304.

Zar, J.H., 1999. *Biostatistical analysis*. Pearson Education India.

Study	Species	Age range	Structure	n	R^2	RMSECV (yr)	% RMSE	Bias	Rank	Wavenumber range
Wedding et al., 2014	*Lutjanus malabaricus*	1-23 yrs	Otolith	169	0.93	1.35	5.8	-0.005	4	7400 – 4000
Rigby et al., 2014	*Squalus megalops*	5-25 yrs	Vertebrae	97	0.89	1.85	7.4	-0.004	4	9300 – 8200 7800 – 6800 4600 - 4000
		5-25 yrs	Dorsal fin spine	97	0.82	2.41	9.6	-0.008	3	9300 – 8200 7800 – 6800 4600 - 4000
		5-25 yrs	Fin clip	97	0.76	2.67	10.7	-0.058	7	9300 – 8200 7800 – 6800 4600 - 4000
	Squalus montalbani	3-31 yrs	Dorsal fin spine	95	0.73	2.96	9.5	0.052	4	9300 – 8200 7800 – 6800 4600 - 4000
Robins et al., 2015	*Lates calcarifer* *	2-12 yrs	Otolith	298	0.86	0.75	6.3	0.300	3	4832 – 4327
	Pagrus auratus *	3-25 yrs	Otolith	306	0.88	1.53	6.1	-0.060	2	6160 – 4580
Rigby et al., 2015	*Sphyrna mokarran*	0.3-10.2 yrs	Vertebrae	76	0.89	0.87	8.5	0.012	5	9200 – 4000
	Carcharhinus sorrah	0.5-9.8 yrs	Vertebrae	99	0.84	0.88	8.9	-0.007	5	9200 – 4000
Helser et al., 2018	*Gadus chalcogrammus*	1-15 yrs	Otolith	202	0.95	0.78	5.2	0.002	--	6821–5269 5022–4171

Table 1. Calibration model results for all previously published FT-NIRS age prediction studies in fish. Unless denoted by *, results were those from the best fit model of the publication for each species. Models denoted with * were full sample models reported for the species. Wavenumber ranges were those incorporated into age prediction models, and were taken from text where specifically outlined by the authors; otherwise,

general ranges were given based upon figures within publications. R^2 = coefficient of determination; RMSECV = Root Mean Square Error of Cross Validation; % RMSE = RMSECV/maximum age included in cross validation model*100; Rank = number of factors in final model.

Calibration Model	Sample size	Rank	R^2	RMSECV	% RMSE	Bias	RPD	Slope	Offset
SA	64	5	0.87	6.62	5.9	-0.127	2.76	0.93	5.23
SA_Teflon	64	2	0.90	5.92	5.3	-0.024	3.08	0.90	7.41
GOM	89	9	0.85	7.52	6.3	-0.034	2.58	0.89	9.71
GOM_Teflon	89	5	0.89	6.31	5.3	-0.019	3.07	0.90	8.83
Combined	153	10	0.88	7.13	5.9	-0.152	2.91	0.92	7.10
Combined Teflon	153	5	0.91	6.08	5.1	-0.042	3.41	0.92	6.72
Combined_Teflon_Calibration	108	5	0.91	6.33	5.3	-0.033	3.28	0.93	6.45
Combined_Teflon_Otolith Weight_Calibration	105	4	0.99	0.001		1.66 e-5	9.51	0.99	0.00
Validation Model	**Sample size**	**Rank**	**R^2**	**RMSEP**		**Bias**	**RPD**	**Slope**	**Offset**
Combined_Teflon_Validation	45	5	0.92	5.61		-0.343	3.64	0.90	8.88
Combined_Teflon_Otolith Weight_Validation	44	4	0.98	0.001		0.001	7.78	0.96	0.00

Table 2. Results of FT-NIRS calibration/validation models for age and otolith weight prediction. SA = South Atlantic; GOM = Gulf of Mexico; Combined = SA and GOM regions combined; Teflon = samples scanned using Teflon aperture; R^2 = coefficient of determination; RMSECV = Root Mean Square Error of Cross Validation; % RMSE = RMSECV/maximum age included in cross validation model*100; Rank = number of factors in final model.

Figure 1. Teflon disk with 2mm aperture aligned over spectrometer window. Otoliths were placed in aperture opening and a transflectance cap placed on top for scanning.

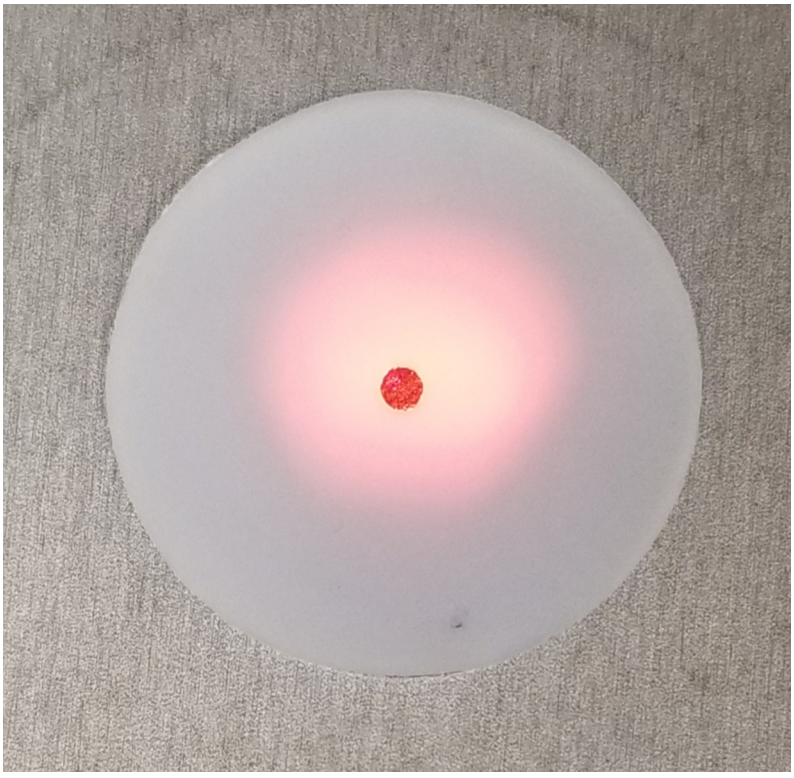

Figure 2. Spectrograms of 153 red snapper otoliths collected with A) no aperture and B) Teflon aperture.

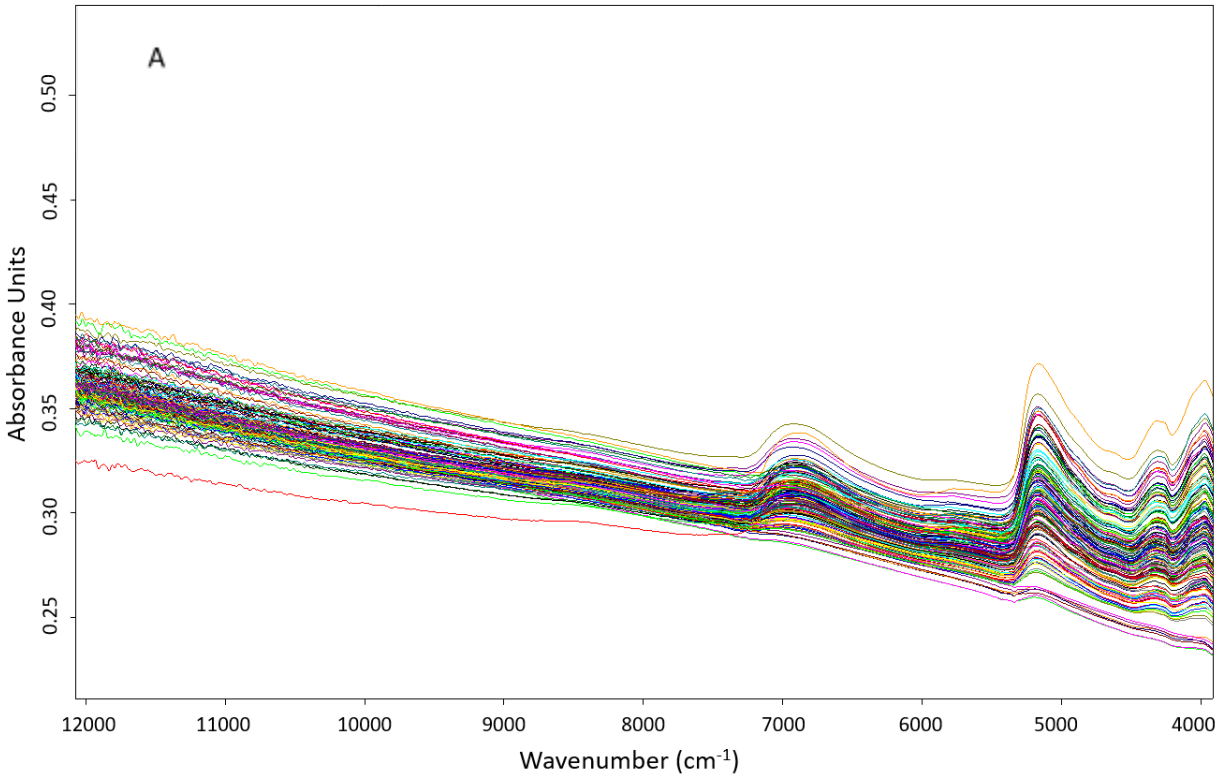

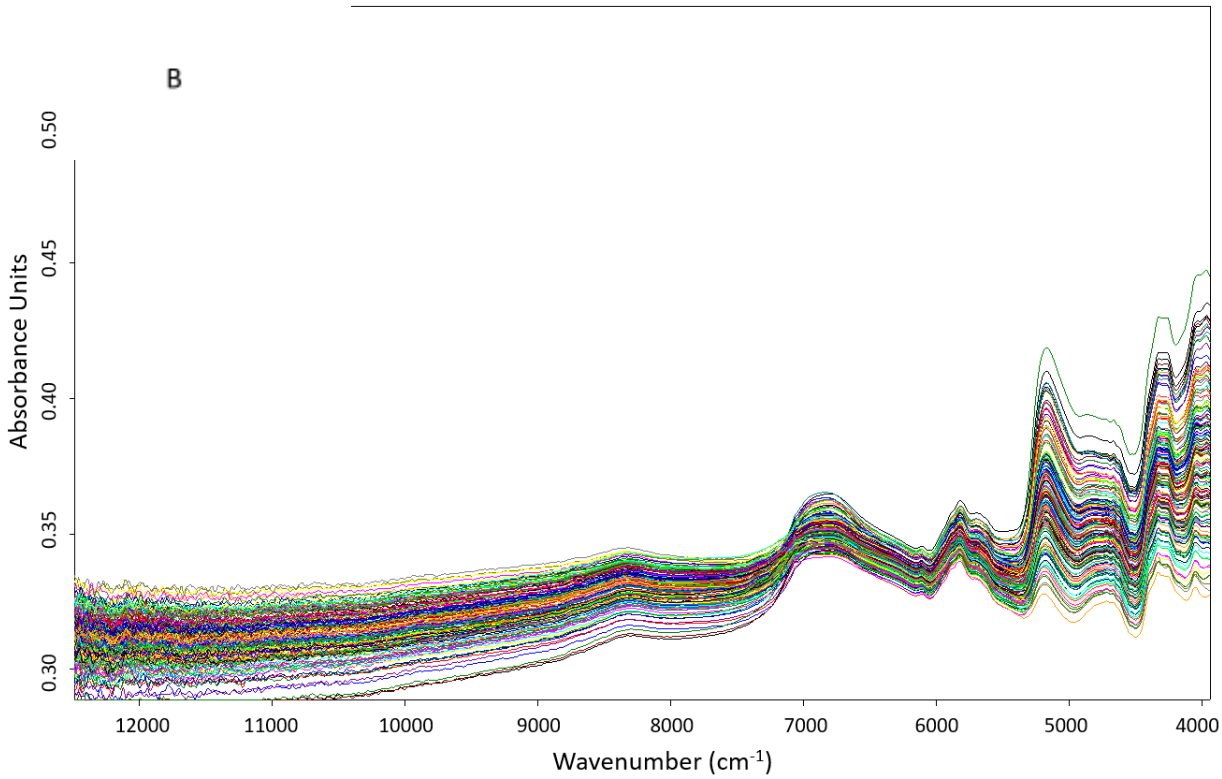

Figure 3: Calibration (black circles) and validation (grey triangles) model results of FT-NIR predicted ages relative to traditional ages. Black line is 1:1 line for reference.

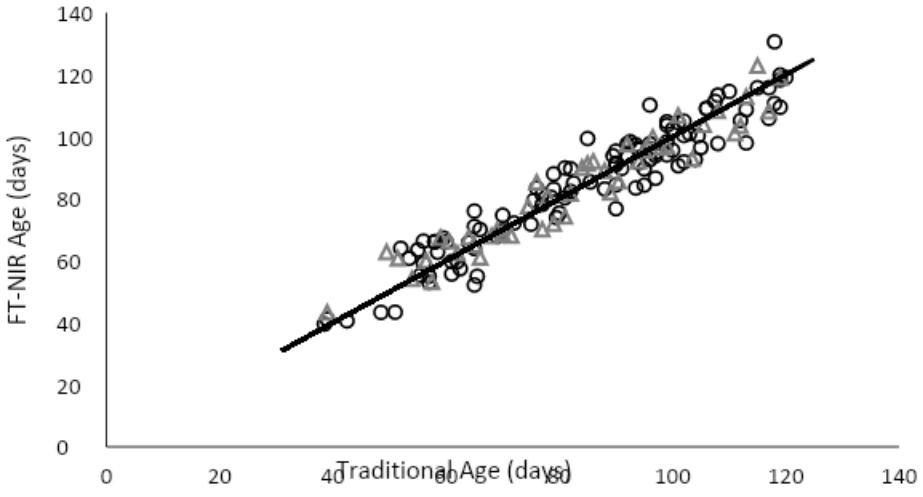

Figure 4. Length-at-age models calculated from traditional (black dashes) and FT-NIRS predicted (grey dashes) ages plotted against observed standard length (SL) at traditional (black circles) and FT-NIRS predicted (grey triangles) ages.

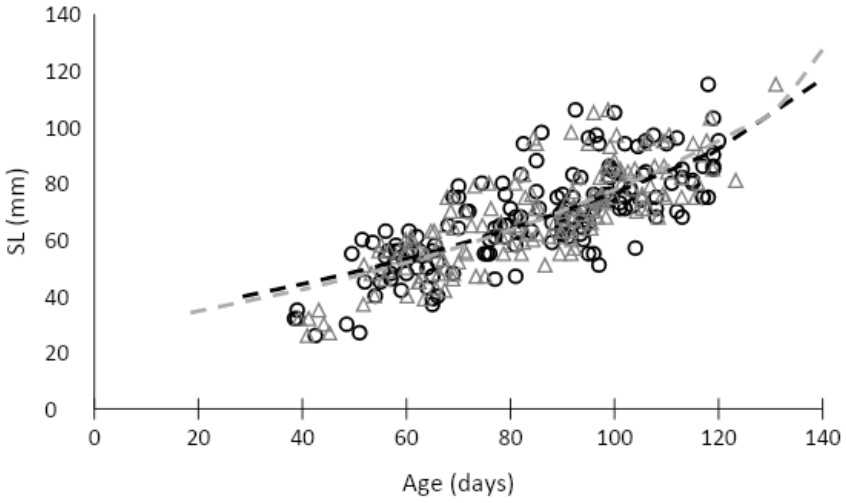

Figure 5. Calibration (black circles) and validation (grey circles) model results of FT-NIR predicted otolith weights relative to directly measured otolith weights. Black line is 1:1 for reference.

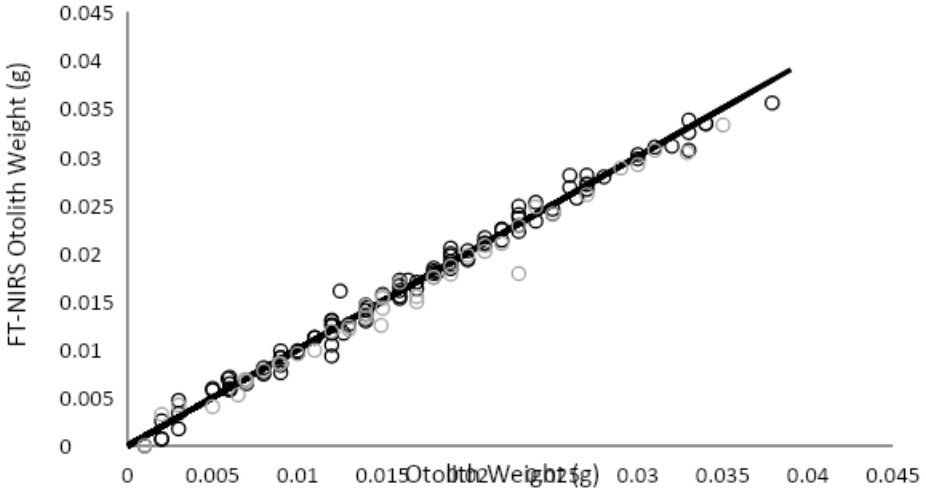

Figure 6. Loadings plots of preprocessed FT-NIRS prediction models corresponding to A) overall regression coefficients for non-apertured (gray line) and Teflon-apertured age (black line) for Combined regional models, and B) Factor 1 loadings for age (black line) and otolith weight (grey line) models for the Combined Teflon model.